Modern Physics Letters B
Vol. 27, No. 26 (2013) 1350189 (10 pages)

DOI: 10.1142/S0217984913501893

A NOVEL GRAPHENE NANO-RIBBON FIELD EFFECT TRANSISTOR WITH SCHOTTKY TUNNELING DRAIN AND OHMIC TUNNELING SOURCE

SEYED SALEH GHOREISHI*
Department of Electrical Engineering, Science and Research Branch, Islamic Azad University, Tehran, Iran
salehghoreyshi@gmail.com

KAMYAR SAGHAFI
Department of Electrical Engineering, Shahed University, P. O. Box 18155-159, Tehran 3319118651, Iran
saghafi@shahed.ac.ir

MOHAMMAD KAZEM MORAVVEJ-FARSHI
Faculty of Electrical and Computer Engineering, Advanced Device Simulation Lab (ADSL), Tarbiat Modares University (TMU), P. O. Box 14115-194, Tehran 1411713116, Iran
farshi_k@modares.ac.ir

Received 10 May 2013
Revised 25 July 2013
Accepted 6 August 2013
Published 9 October 2013

In this paper, we propose a novel tunneling graphene nanoribbon field effect transistor by modification of the conventional structure in a way that its drain high-doped extension part is replaced by lightly linear doped region. Then the proposed structure has a Schottky contact at the drain side. As the source contact is ohmic and the drain contact is Schottky, this structure is called Schottky–Ohmic tunneling graphene nanoribbon field effect transistor. Electrical behaviors of the proposed device are investigated by mode space nonequilibrium Green's function (NEGF) formalism in the ballistic limit. Simulation results show that without increasing transistor length, I_{OFF}, I_{ON}/I_{OFF}, ambipolar behavior, delay time and PDP of the proposed structure improve, in comparison with the conventional tunneling graphene nanoribbon field effect transistor with the same dimension. Also subthreshold swing which is one of the evident characteristics of the tunneling FET is preserved in this structure.

Keywords: Ambipolar; BTBT; Schottky; T-GNRFET; NEGF.

*Corresponding author.

1. Introduction

Due to steady scaling down of transistors and reaching the nano-dimensions, it seems necessary to introduce new materials instead of silicon which can be made in these dimensions and have high stability and proper electrical properties. Graphene is one of these materials, which has almost ballistic property and very high mobility and velocity saturation, like carbon nanotube, but it has zero energy gap.[1–3] Thus, it is not suitable for being used in the channel of the field effect transistors.

By cutting graphene and converting it to graphene nanoribbon (GNR), energy gap is made. Energy gap is tunable in GNR and increases with the decrease in width of nanoribbon.[4,5] Recent experiments has shown that all GNRs with width of less than 10 nanometers have nonzero energy gap and are suitable for being used in the channel of field effect transistors.[6] Tunable property of energy gap with nanoribbon width makes this material very suitable for the channel of field effect transistors.

GNR based transistors can be classified into three groups;[7–12] the first one called Schottky barrier graphene nanoribbon field effect transistor (SB-GNRFET) which is simply created by connecting two metals as the source and the drain to both sides of a GNR channel and the current is controlled through the gate and by changing Schottky barrier height on both sides of the channel. Another type is conventional or MOS like graphene nanoribbon field effect transistor (MOS-like-GNRFET) which is created by connecting two heavily doped regions of P^+ or N^+ on both sides of the intrinsic channel as the source and the drain ($N^+ - I - N^+$ or $P^+ - I - P^+$). In these transistors, contacts are ohmic and like conventional FETs, modulation of current is done by the gate with varying the height of the barrier in the channel region. The third group is tunneling graphene nanoribbon field effect transistors (T-GNRFET) which have $P^+ - I - N^+$ structure and its only structural difference from the second model is in the type of source region. Current mechanism in these transistors is based on band-to-band tunneling (BTBT); hence, they have very suitable subthreshold swing. For this reason, they are appropriate for high speed circuits with low static power dissipation.[13] Unlike SB-GNRFETs, two heavily-doped regions are used on both the source and the drain sides in T-GNRFETs and contacts on both the source and the drain sides are ohmic. Like SB-GNRFETs and MOS-like GNRFETs, T-GNRFETs have improper ambipolar property, due to the contribution of both holes and electrons in the current. Suitable subthreshold swing is one of the evident characteristics of tunneling transistors, which should be preserved in the proposed structures.

Many works have been done to improve ambipolar behavior in MOS-like-CNT (GNR) FET.[14–19] Unfortunately, the device length has increased in most of them. So far, no considerable work has been done on T-GNRFETs which can modify its ambipolar behavior. In this paper, a new structure is presented in which ambipolar behavior, I_{OFF}, $I_{\mathrm{ON}}/I_{\mathrm{OFF}}$, delay ($\tau$) and PDP considerably improved by simply modifying the structure of conventional T-GNRFET without increasing transistor length. In addition, subthreshold swing which is one of the evident characteristics

of tunneling transistors remained almost unchanged. This new structure is called Schottky–Ohmic T-GNRFET (SO-T-GNRFET).

In Sec. 2, the proposed structure is introduced and simulation procedure is explained. Then, in Sec. 3, simulation results accompanied with discussions are given and, finally, conclusions are made in Sec. 4.

2. The Proposed Structure and Simulation Method

The proposed structure is shown in Fig. 1. Figure 1(a) demonstrates the conventional T-GNRFET structure and Fig. 1(b) presents SO-T-GNRFET. In the new structure, a high concentration region is used on the source side. Length of this region is 10 nm and its doping concentration is equal to 10^{-2} (dopant/atom). Work functions of the source contact and the gate metal are equal to the work function of the graphene nanoribbon. The channel region is intrinsic and its length is 20 nm.

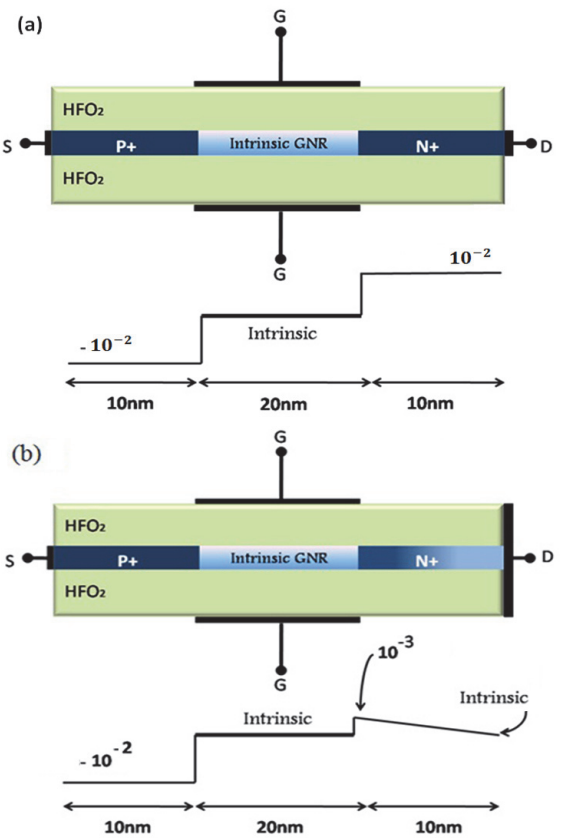

Fig. 1. The cross section and doping profile of (a) T-GNRFET and (b) SO-T-GNRFET. A HFO_2 dielectric layer with $\epsilon_{ox} = 16$ and $t_{ox} = 1.5$ nm is used. The source region is doped with 10^{-2} (dopant/atom) P type impurities. The linear-doped region is doped from 10^{-3} (dopant/atom) N type impurities at the gate side to zero at the drain side.

On the drain side, instead of using a highly doped region, a 10 nm but lightly doped region, where doping linearly decreases from 10^{-3} (dopant/atom) to intrinsic, is applied. This lightly doped region decreases the parasitic capacitance. Work function of the drain metal is selected so that the drain fermi level places 0.2 eV above the bottom of the conduction band on the drain side. Since the proposed structure has ohmic contact on the source side and Schottky contact on the drain side, therefore, it is called Schottky–Ohmic Tunneling GNR Field Effect Transistor. The nanoribbon is selected of armchair type with $n = 3p + 1 = 16$ and $W(width) = 1.84$ nm, with $E_g = 0.7$ eV. Dielectric layer is made of HFO_2 with $\epsilon_{ox} = 16$ and thickness of 1.5 nm.

We solved the Schrödinger and Poisson equations self-consistently using the nonequilibrium Green's function (NEGF) method in the mode space approach to save time and computational cost. We have considered two subbands for this investigation. To solve Schrödinger equation, the Green's function must be calculated according to the following formula:

$$G(E) = [(E - i0^+)I - H - \Sigma_S(E) - \Sigma_D(E)]^{-1}, \tag{1}$$

where I is an identity matrix, E is the energy, H is Hamiltonian matrix, $\Sigma_S(E)$ and $\Sigma_D(E)$ are self-energy matrices of the source and the drain, respectively. The first step in NEGF procedure is calculation of the Hamiltonian of the structure using suitable basis functions for the channel in the isolated state.[20] In this step, the potential distribution obtained from Poisson equation solution is also entered in NEGF formalism. Hamiltonian is calculated by tight-binding method and only orbital of p_z. Like CNT, considering only one orbital p_z to investigate carrier transport in nanoribbon will suffice because orbitals p_z almost entirely are uncoupled compared to other orbitals and states including orbitals s, p_x and p_y are much lower or higher than Fermi energy level and consequently they do not have a considerable responsibility in carriers transport.[21]

Unlike CNT, presence of edge in GNR necessitates considering effect of the edge bond relaxation and third nearest neighbor interaction.[20] The third nearest neighbor interaction is much weaker than the first nearest neighbor interaction but could influence the transistor's performance.[20] Third nearest neighbor coupling parameter is considered with $t_3 = 0.2$ eV in our work.

Hamiltonian matrix of subband q which calculated by tight-binding approximation with only one orbital is:

$$H_q = \begin{bmatrix} U_1 & b_{2q} & 0 & t_3 & & \\ b_{2q} & U_2 & b_{1q} & 0 & & \\ 0 & b_{1q} & U_3 & b_{2q} & 0 & t_3 \\ t_3 & 0 & b_{2q} & U_4 & b_{1q} & 0 \\ & & 0 & b_{1q} & U_4 & \ddots \\ & & t_3 & 0 & \ddots & \ddots \end{bmatrix}, \tag{2}$$

where U_i, $b_{1q} = t_0(1 + 4C_{\text{edge}} \sin^2(\pi q/(n+1))/(n+1))$, $b_{2q} = 2t_0 \cos(\pi q/(n+1))$, $t_0 \approx 2.7$ eV and $C_{\text{edge}} = 0.12$ are on-site electrostatic potential at the ith GNRs ring or at the column i, hopping parameter between two closer and two further nearest neighboring GNR rings or columns, the hopping parameter between two adjacent carbon atoms and the edge bond relaxation parameter, respectively.[20]

In the next step, the matrices related to self-energy contacts, which indicate coupling of the channel to the drain and the source contacts, should be calculated. Σ_S can be calculated by the method introduced in Ref. 20. In this case, we group each of the two atoms together as a new cell, the coupling between adjacent new cell can be described by a 2×2 matrix. Each new cell only couples to its nearest neighbors. Then self-energy matrix can be solved by an iterative method. In order to reduce simulation time, one can use Sanch–Rubio iterative method.[23]

The contact of the drain side is Schottky. In order to calculate the self-energy of the drain contact, the method introduced by Guo *et al.* is used in Ref. 22. Σ_D has only one nonzero element of $\Sigma_D(N, N)$ as can be calculated using the following relation:

$$\Sigma_D(N,N) = \frac{(E - U_N) - \sqrt{(E - U_N)^2 - 4b_{1q}^2}}{2}. \tag{3}$$

The current of the device is computed by:

$$I_{DS} = \frac{2e}{h} \int_{-\infty}^{\infty} T(E)(F(E - E_{FS}) - F(E - E_{FD}))dE \tag{4}$$

where $T(E) = \text{trace}(\Gamma_S G \Gamma_D G^+)$ represents transmission probability of a carrier with energy of E between two contacts and Γ is broadening matrix.

3. Simulation Results

Using the procedure which explained in the previous section, I_{DS}–V_{DS} and I_{DS}–V_{GS} characteristics of the proposed structure were simulated. The results along with a comparison between proposed device and conventional T-GNRFET with the same structure are presented in Figs. 2 and 3. Figure 2 shows I_{DS}–V_{DS} characteristic for the specified gate voltage. Due to similarity of the band structure on the source side, both structures have almost equal current. In Fig. 3, a comparison is shown between I_{DS}–V_{GS} characteristic in SO-T-GNRFET and T-GNRFET for various V_{DS}. In the proposed structure, ambipolar behavior is considerably modified and I_{OFF} reduced by about 2 orders of magnitude. In order to justify this improvement, we calculate the energy band structure and the number of electrons per unit energy along the device in OFF state, i.e. $V_{GS} = -0.4$ V and $V_{DS} = 0.4$ V, which is shown in Fig. 4. Figure 4(a) is related to T-GNRFET and Fig. 4(b) to SO-T-GNRFET. As shown in the figures, it can be found that in the SO-T-GNRFET, width of tunneling region increased on the drain side. In fact, a barrier is created against carriers which want to tunnel from the channel to the drain side, using a lightly doped region on the drain side, and consequently I_{OFF} decreases. As mentioned above, since I_{ON} results

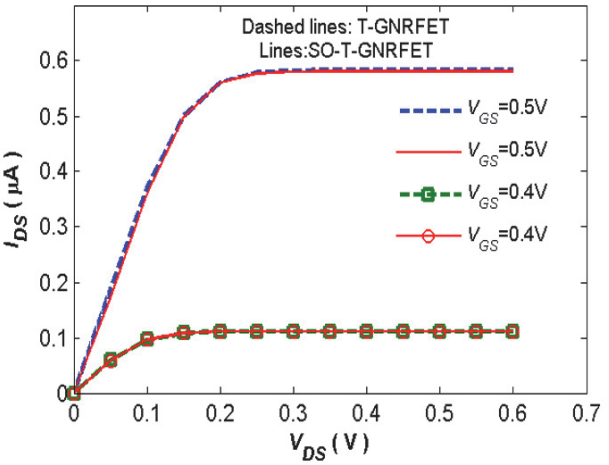

Fig. 2. (Color online) Comparision of I_{DS}–V_{DS} characteristics obtained by SO-T-GNRFET (lines) and T-GNRFET (dashed lines) for various V_{GS}.

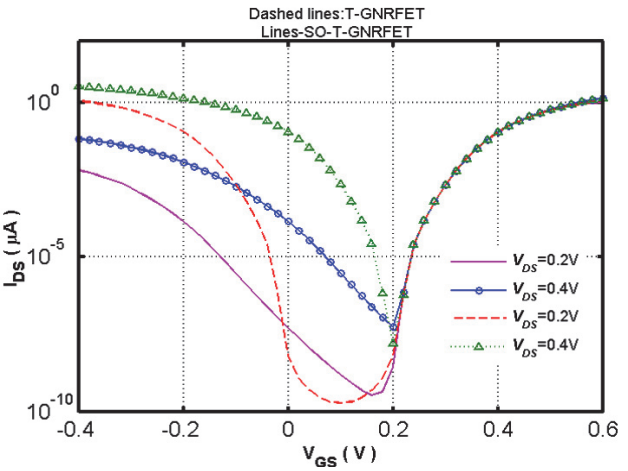

Fig. 3. (Color online) Comparision of I_{DS}–V_{GS} characteristics obtained by SO-T-GNRFET (lines) and T-GNRFET (dashed lines) for various V_{DS}.

from band to band tunneling from the source to the channel in tunneling devices and considering that the energy band structure in the source side did not change in SO-T-GNRFET, therefore, no considerable change could be seen in I_{ON} and also subthreshold swing, as one of the evident characteristics of tunneling transistors, was not degraded.

For more comparison, ratio of $I_{\mathrm{ON}}/I_{\mathrm{OFF}}$ in terms of I_{ON} for $V_{DS} = 0.4$ V is shown in Fig. 5. In order to draw this figure, the procedure introduced in Ref. 18 is used. It can be found from the figure that SO-T-GNRFET has much higher $I_{\mathrm{ON}}/I_{\mathrm{OFF}}$ than T-GNRFET, even in low I_{ON}. The reason is that I_{ON} is almost

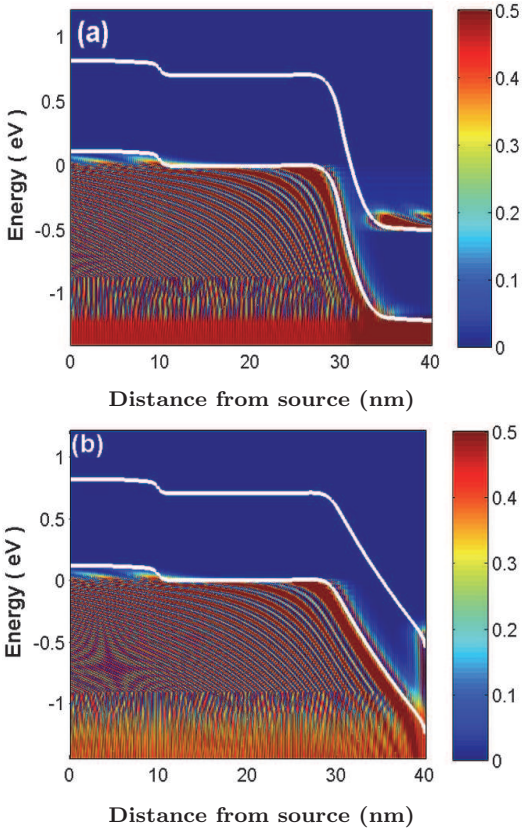

Fig. 4. (Color online) The band structure (white lines) and the number of electrons per unit energy (color bar) along the devices at $V_{DS} = 0.4$ V and $V_{GS} = -0.4$ V for (a) T-GNRFET and (b) SO-T-GNRFET.

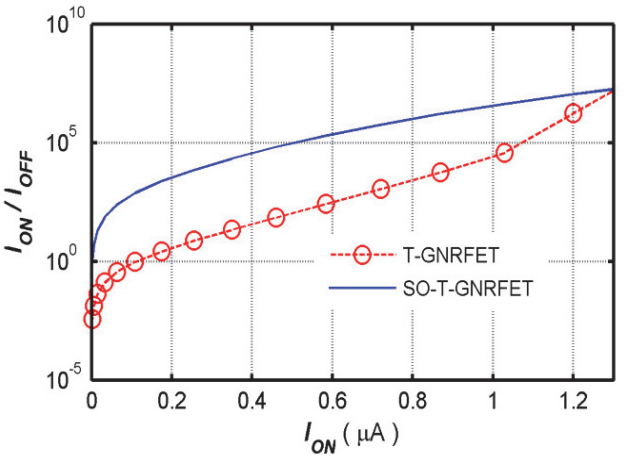

Fig. 5. (Color online) $I_{\rm ON}/I_{\rm OFF}$ ratio versus $I_{\rm ON}$ for SO-T-GNRFET (lines) and T-GNRFET (dashed lines) at $V_{DS} = 0.4$ V.

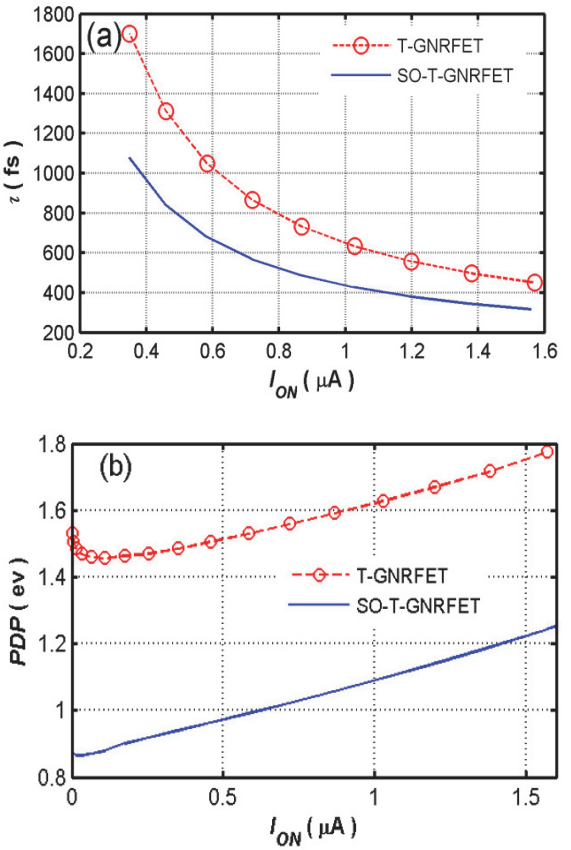

Fig. 6. (a) Delay time and (b) power-delay product versus I_{ON} for two structures at $V_{DS} = 0.4$ V.

equal in both structures but I_{OFF} more decreases in SO-T-GNRFET. Since ratio of $I_{\mathrm{ON}}/I_{\mathrm{OFF}}$ in SO-T-GNRFET is suitable in low I_{ON}, therefore, this structure could be used in ultra low power application. Two key parameters for studying behavior of the device are delay time (τ) and power delay product (PDP) at the time of switching (indicating consumed energy at every time of switching) which was obtained from the following relations:[18]

$$\tau = (Q_{\mathrm{ON}} - Q_{\mathrm{OFF}})/I_{\mathrm{ON}}\,, \tag{5a}$$

$$PDP = (Q_{\mathrm{ON}} - Q_{\mathrm{OFF}})V_{DD}\,. \tag{5b}$$

In the above relations, Q_{ON} and Q_{OFF} are the total charges of the device, including the source and the drain regions, at ON and OFF states, respectively. Figure 6 shows these two parameters in terms of I_{ON} in $V_{DS} = 0.4$ V for T-GNRFET and SO-T-GNRFET. According to the figure, the proposed structure has lower PDP and delay time (τ). This comparison indicates that the proposed structure could be more appropriate than the other one for being used in low power

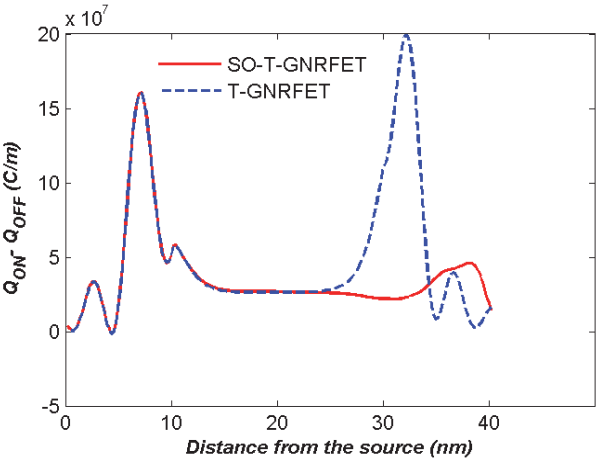

Fig. 7. (Color online) $\Delta Q = Q_{\mathrm{ON}} - Q_{\mathrm{OFF}}$ along the device for SO-T-GNRFET (lines) and T-GNRFET (dashed lines).

and high speed applications. The reason for decrease of τ and PDP in the proposed structure is due to using a linear doped region, of course, with a drain lightly doped region, which acts as a spacer region between contacts of the gate and the drain. Therefore, parasitic capacitance decreases and variation of the gate voltage leads to less charge variation inside the channel and, as a result, Q_{ON} and Q_{OFF} decreases. Figure 7 shows comparison of $\Delta Q = Q_{\mathrm{ON}} - Q_{\mathrm{OFF}}$ in SO-T-GNRFET and T-GNRFET. As it can be seen in the figure, ΔQ in SO-T-GNRFET is much less than T-GNRFET at the drain side (30 nm). As a result, we expect to reduce the parasitic capacitances.

Considering the direct relationship of Q_{ON} and Q_{OFF} with PDP, as is evident in the Fig. 6(b), PDP decreases as well. In other words, volume of the charges which should be replaced from ON to OFF states or vice versa inside the transistor decreases in the proposed structure.

4. Conclusion

The NEGF formalism with an uncoupled mode space approach has been used to investigate electrical properties of a modified T-GNRFET, namely, "SO-T-GNRFET" and simulated characteristics have been compared with those of conventional T-GNRFETs. Without increasing the transistor length, by using lightly and linearly decreased doping concentration profile at the drain side, leakage current of SO-T-GNRFET decreased considerably. The simulation results demonstrated that the proposed structure had higher $I_{\mathrm{ON}}/I_{\mathrm{OFF}}$ ratio, the same I_{ON} current and subthreshold swing. Also this structure enjoyed from improved switching behavior like PDP and delay. All of these cases made the proposed structure appropriate for being used in low power and high speed applications.

References

1. K. Novoselov *et al.*, *Science* **306** (2004) 666–669.
2. Y. Zhang, Y. W. Tan, H. L. Stormer and P. Kim, *Nature* **438** (2005) 201–204.
3. C. Berger *et al.*, *Science* **312** (2006) 1191–1196.
4. M. Eazwa, *Phys. Rev. B: Condens. Matter* **73** (2006) 045432–045439.
5. Y. W. Son, M. L. Cohen and S. G. Louie, *Phys. Rev. Lett.* **97** (2006) 216803–216806.
6. X. Li, X. Wang, L. Zhang, S. Lee and H. Dai, *Science* **39** (2008) 1229–1232.
7. Y. Yoon, G. Fiori, S. Hong, G. Iannaccone and J. Guo, *IEEE Trans. Electron Dev.* **55** (2011) 2314–2320.
8. G. Liang, N. Neophytou, M. Lundstrom and D. Nikonov, *J. Appl. Phys.* **107** (2007) 054307–054313.
9. Y. Ouyang, Y. Yoon and J. Guo, *IEEE Trans. Electron Dev.* **54** (2007) 2223–2228.
10. S. K. Chin, D. Seah, K. Lam, G. S. Samudra and G. Liang, *IEEE. Trans. Electron Dev.* **57** (2010) 3144–3152.
11. P. Zhao, J. Chauhan and J. Guo, *Nano. Lett.* **9** (2009) 684–688.
12. A. A. Orouji and Z. Arefinia, *Phys. E: Low. Dimens. Syst. Nanostruct.* **41** (2009) 552–557.
13. W. Y. Choi, B. G. Park, J. D. Lee and T. J. K. Liu, *IEEE Trans. Electron Dev. Lett.* **28** (2007) 743–751.
14. R. Yousefi, K. Saghafi and M. K. Moravvej-Farshi, *IEEE Trans. Electron Dev.* **57** (2010) 765–771.
15. I. Hassaninia, M. H. Sheikhi and Z. Kordrostami, *Solid State Elect.* **52** (2008) 980–985.
16. D. Unluer, F. Tseng, A. W. Ghosh and M. R. Stan, *IEEE Trans. Nanotech.* **10** (2011) 931–938.
17. R. Yousefi and S. S. Ghoreyshi, *J. Mod. Phys. Lett. B* **26** (2012) 1250096-1–1250096-9.
18. J. Guo, A. Javey, H. Dai and M. Lundstrom, *IEDM Tech. Dig.* (2004) 703.
19. A. Naderi, P. Keshavarzi and A. Orouji, *Superlattices Microstruct.* **50** (2011) 145–156.
20. P. Zhao and J. Guo, *J. Appl. Phys.* **105** (2008) 034503-1–034503-7.
21. J. Guo, Ph.D. thesis, Purdue University (2004).
22. J. Guo, S. Datta, M. P. Anantram and M. Lundstrom, *J. Comp. Elect.* **3** (2004).
23. M. P. L. Sancho, J. M. L. Sancho and J. Rubio, *J. Phys. F. Met. Phys.* **15** (1984) 851–858.